

Scoring personalized molecular portraits identify Systemic Lupus Erythematosus subtypes and predict individualized drug responses, symptomatology and disease progression

Daniel Toro-Domínguez , Jordi Martorell-Marugán , Manuel Martínez-Bueno, Raúl López-Domínguez, Elena Carnero-Montoro, Guillermo Barturen, Daniel Goldman, Michelle Petri, Pedro Carmona-Sáez [†] and Marta E. Alarcón-Riquelme[†]

Corresponding author: Daniel Toro-Domínguez, Daniel.toro@genyo.es. Tel: +34 958715500-143.

[†]The last two authors should be regarded as Joint Last Authors.

Abstract

Objectives: Systemic Lupus Erythematosus is a complex autoimmune disease that leads to significant worsening of quality of life and mortality. Flares appear unpredictably during the disease course and therapies used are often only partially effective. These challenges are mainly due to the molecular heterogeneity of the disease, and in this context, personalized medicine-based approaches offer major promise. With this work we intended to advance in that direction by developing MyPROSLE, an omic-based analytical workflow for measuring the molecular portrait of individual patients to support clinicians in their therapeutic decisions.

Methods: Immunological gene-modules were used to represent the transcriptome of the patients. A dysregulation score for each gene-module was calculated at the patient level based on averaged z-scores. Almost 6100 Lupus and 750 healthy samples were used to analyze the association among dysregulation scores, clinical manifestations, prognosis, flare and remission events and response to Tabalumab. Machine learning-based classification models were built to predict around 100 different clinical parameters based on personalized dysregulation scores.

Results: MyPROSLE allows to molecularly summarize patients in 206 gene-modules, clustered into nine main lupus signatures. The combination of these modules revealed highly differentiated pathological mechanisms. We found that the dysregulation of certain gene-modules is strongly associated with specific clinical manifestations, the occurrence of relapses or the presence of long-term remission and drug response. Therefore, MyPROSLE may be used to accurately predict these clinical outcomes.

Conclusions: MyPROSLE (<https://myprosle.genyo.es>) allows molecular characterization of individual Lupus patients and it extracts key molecular information to support more precise therapeutic decisions.

Keywords: Systemic Lupus Erythematosus, autoimmune diseases, computational models, molecular profiling, personalized medicine

Introduction

Systemic Lupus Erythematosus (SLE) is a heterogeneous autoimmune disease with a nonlinear clinical course and unpredictable patterns of flares and remissions with involvement of a wide range of tissues and organs [1]. SLE causes significant suffering and mortality, and with

only three new FDA-approved SLE therapies in 65 years, there is a large unmet need to develop new and effective therapeutic approaches [2, 3]. One contributing cause of treatment failure is the heterogeneous dysregulation of molecular mechanisms that are uncharacterized at the individual patient level [4]. A large proportion of

Raul López Domínguez: He is a biologist and bioinformatician with expertise in big data applied to immunology.

Jordi Martorell-Marugán: He is a researcher focused on the development of omics data analysis and integration methods and their application to complex disease data.

Manuel Martínez-Bueno: He is a researcher focused on genetic analysis applied to complex diseases.

Daniel Toro Domínguez: He specialized in computational biology applied to the study of autoimmune diseases, omics data analysis, machine learning and molecular clustering analysis.

Elena Carnero-Montoro: She is a researcher specialized in genetic epidemiology and epigenomics.

Guillermo Barturen: He is a researcher with computational expertise on high-throughput technologies analysis.

Daniel Goldman: He is a professor of medicine specialized in autoimmune diseases.

Michelle Petri: She is a professor of medicine specialized in autoimmune diseases.

Pedro Carmona-Sáez: He is a professor of biostatistics with computational expertise in bioinformatics.

Marta E. Alarcón-Riquelme: She specialized in the genetics of complex diseases and autoimmunity.

Received: March 7, 2022. Revised: July 4, 2022. Accepted: July 21, 2022

© The Author(s) 2022. Published by Oxford University Press.

This is an Open Access article distributed under the terms of the Creative Commons Attribution Non-Commercial License (<https://creativecommons.org/licenses/by-nc/4.0/>), which permits non-commercial re-use, distribution, and reproduction in any medium, provided the original work is properly cited. For commercial re-use, please contact journals.permissions@oup.com

patients show none or partial response to therapies, which are prescribed based on a trial-and-error approach that clearly requires improvement [5].

It is during periods of disease activity, either chronic or flares, when organs suffer most damage. Disease activity indexes, such as the SLE Disease Activity Index (SLEDAI), the British Isles Lupus Assessment Group Index (BILAG) or the Physician Global Assessment (PGA), are used by clinicians as a support for the immediate therapeutic decision [6, 7]. These indexes are based on a summation of organ manifestations, sometimes in a weighted fashion. An equal activity index value can be generated by different combinations of manifestations, thus hindering systematic comparisons across patients. In addition, activity indexes do not reflect the molecular portrait of the patients, that is, the dysregulated biological pathways and molecular mechanisms associated with the disease status, which may also be different between patients and even throughout the course of the disease. The molecular portrait impacts on the clinical manifestations and the response to drugs. Currently, the use of personalized therapies based on molecular information is advanced in some diseases, such as cancer [8–10], and it is considered a promising strategy to overcome disease heterogeneity. However, in autoimmunity, individualized prescription of therapies based on molecular patterns does not exist for routine clinical care, mainly due to the lack of specific and easy-to-use tools for these purposes.

Despite this, there is an increasing interest to address such heterogeneity both in autoimmunity [11–13] as in SLE specifically through molecular stratification [14–16] and biomarker discovery for specific conditions [17]. While stratification studies have shown how different molecular patterns reflect different phenotypes, clustering results depend on technical variables such as the cohort features, the sample sizes and the statistical approaches used. For this reason, numerous cross-sectional clustering studies often obtain different subgroups of patients. In addition, studies are mostly exploratory and they are not intended for a direct clinical practice application. On the other hand, many clinical and omics-based markers for different clinical outcomes have been identified using machine learning (ML) techniques. However, clinical markers are often subject to enormous variability across patients, and omics experiments are often not validated in external cohorts due to the enormous biases caused by the use of different technical platforms [18]. Therefore, it is necessary to analyze in detail the connections between the molecular portraits and their implications in the medical environment, but also to use a standardized approach to incorporate this knowledge in practice reproducibly.

In this multi-cohort study, we sought to define the relevant connections between personalized molecular portraits and consequent medical implications in order to predict drug response, disease course, remissions and flares and clinical manifestations. For this goal, a

new scoring system capable of measuring the personalized Molecular dYsregulated PROfiles of SLE patients (MyPROSLE) was developed, which allows relatively simple identification and standardized quantification of the molecular fingerprints that drive the SLE activity in individual patients. Interestingly, two clearly differentiated SLE subtypes at the clinical and molecular level were identified and their stability over time was assessed, which supports different pathological mechanisms. Finally, a web tool to easily assess SLE molecular portraits from transcriptome information through MyPROSLE in individual patients has been developed. Figure 1 shows a general scheme of the different steps of the workflow.

Materials and Methods

SLE datasets and data pre-processing

Genome-wide gene expression levels and clinical and demographic information (when available) for nine datasets (six and three cross-sectional and longitudinal datasets, respectively) were downloaded from the National Center for Biotechnology Information (NCBI) Gene Expression Omnibus (GEO) database [19]. We also included the dataset from the PRECISESADS project [12]. Datasets were used for different purposes depending on the information they contain, as detailed in Table 1. The clinical data of the patients from the GSE121239 cohort were provided by Johns Hopkins University School of Medicine. Clinical drug response indices to Tabalumab for patients from the GSE88887 [20] dataset were collected by Eli Lilly and Company (ClinicalTrials.gov Identifiers NCT01205438 and NCT01196091).

Raw data from each dataset were processed following a platform-specific workflow, as described in Martorell-Marugán et al. [21]. Expression data were transformed to logarithmic scale and transcripts were annotated from probes to gene symbol for each dataset. Duplicated genes were merged assigning their mean expression value and genes with zero or near to zero variance were filtered using caret R package (version 6.0–91, 22).

In summary, 10 different cohorts comprising a total of 6134 whole blood SLE samples and 757 healthy controls were collected.

MyPROSLE score

Most genes form regulatory networks, acting as gene-modules in specific biological functions and are likely co-expressed. Based on this principle, we summarized individual gene expression into 606 co-expressed gene modules that regulate biological and immunological mechanisms previously described by Li et al. [23] and Chaussabel et al. [24]. Genes and gene-module connections were obtained from tmod R package (version 0.46.2) [25]. This process reduced the dimensionality by projecting thousands of genes into 606 functional gene-modules.

Next, a score for each gene-module was calculated to quantify the dysregulation of each function for individual patients compared with the healthy state. For this, we

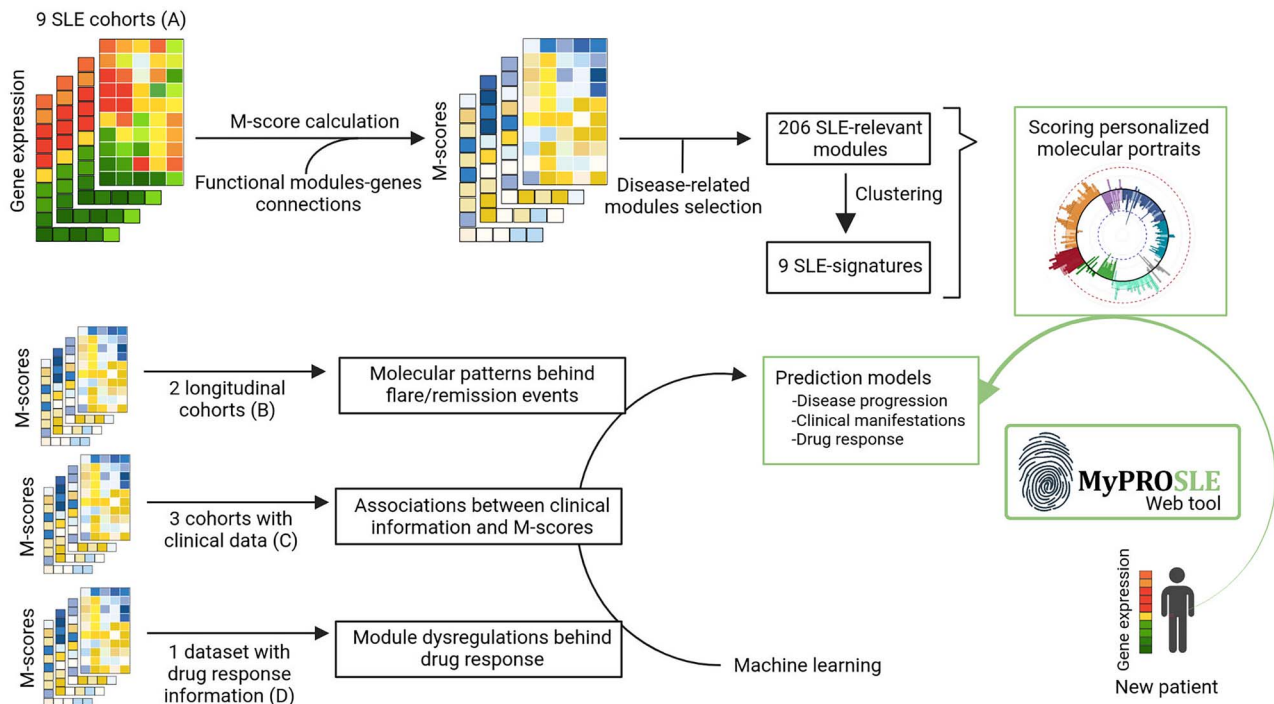


Figure 1. Summary of the main steps of the workflow. First, the M-scores for immune related gene-modules are calculated for nine different cohorts, those relevant to the disease were selected and clustered into nine main SLE-signatures that reflect nine well-differentiated biological functions. Secondly, different approaches were carried out relating the molecular profiles with different clinical outcomes, and predictive models were built for each of them. Finally, a web tool was developed to calculate the M-scores and apply the prediction models on new patient samples.

Table 1. Description of datasets used in the study

Dataset ID	SLE samples	Healthy samples	Data description	Used for
GSE45291 [45]	292	20	One gene expression sample per patient	A
GSE61635	79	30	RNP autoantibody+ SLE samples	A
GSE72509 [46]	99	18	One gene expression sample per patient	A
GSE108497	325	187	Samples taken during pregnancy	A
GSE110169 [47]	82	77	One gene expression sample per patient	A
GSE110174 [47]	144	10	One gene expression sample per patient	A
GSE65391 [14]	924	72	158 pediatric longitudinal SLE patients and 48 age-matched controls	A, B, C
GSE121239 [15]	727	20	301 adults longitudinal SLE patients and 20 healthy controls	A, B, C
GSE88887 [20]	3086	60	3 follow-up points of patients treated with Tabalumab or placebo	D
PRECISESADS [12]	376	263	Genotyped and fully clinically characterized patients.	A, C

(A) Datasets used for MyPROSLE system construction, selection of SLE-related gene-modules and clustering of gene-modules and patients. (B) Datasets used for longitudinal and time-dependent analysis and for the construction of predictive models for future disease flares. (C) Datasets used for measure the association between molecular portraits and clinical manifestations and for the construction of predictive models for clinical variables. (D) Dataset used for drug response analysis and for drug response prediction models construction.

adapted the methodology developed by Meche *et al.* [26]. Briefly, for each patient, the z-score of the expression of each gene was calculated with respect to the expression of the gene in a pool of healthy controls (from the same dataset). Then, the score for a gene-module i (M-score i) was computed as the mean of the z-scores of all its genes, as shown in Equation 1:

$$Mscore_i = \frac{\sum_{j=1}^{n_i} \left(\frac{x_j - \mu_{jH}}{\sigma_{jH}} \right)}{n_i} \quad (1)$$

where x_j is the expression of gene j in an individual patient, μ_{jH} and σ_{jH} are the mean of the expression and

the standard deviation of gene j in healthy samples and n_i is the number of genes from the module i . The M-scores follow a centered normal distribution given that it is a mean of z-scores. The interval of 1.65 and -1.65 in such distribution contain 90% of the data, which correspond to a P -value of 0.05 for each tail [27]. Therefore, we can consider statistically significant those M-scores that take values greater than 1.65 or less than -1.65 .

Next, only those gene-modules that could be related to the disease were selected. For this aim, the gene-modules that did not achieve significantly high M-scores in at least 10% of the samples and at least three of the nine datasets were removed. This selection step allowed to retain gene-modules that, on the one hand, may appear

in small subsets of patients, but on the other hand, do so recurrently between studies, dealing with potential biases caused by individual studies. Finally, 206 gene-modules were selected. In order to test the consistency of M-scores, multiple random sampling of healthy controls was applied to each dataset to generate various subsets (100 subsets for each dataset and sample size, ranging from 90 to 10% of the total healthy samples) and M-scores of patients were recalculated among subsampling.

In summary, MyPROSLE system summarizes the molecular portrait of a patient by measuring dysregulation scores (or M-scores) for 206 functional gene-modules with respect to healthy distribution.

Measuring M-scores without healthy samples

One of the strengths of MyPROSLE is that it may calculate the M-scores without providing healthy controls data using our standardized reference of SLE samples. Such SLE reference was built using the SLE samples from our datasets and the genes within the 206 gene-modules. Each patient is individually normalized by centering the mean of the selected genes and dividing it by its standard deviation. The M-scores of these patients have been previously calculated with respect to their controls. To analyze a new patient, first, their expression is centered and scaled. Then, patient–patient similarity between the provided sample and the reference SLE samples is measured using the Euclidean distance. The M-scores for the new patient are calculated as the mean of the M-scores of the k most similar SLE samples of the reference (Supplementary Figure 1). In this way, we can estimate the dysregulation score of each gene-module in a patient, without the need of new healthy individuals profiling and avoiding potential variations in the M-scores calculation due to the use of different healthy references. This system was tested using the patients from one of the datasets (GSE61635), not included in the reference, and measuring the correlation between the M-scores calculated with respect to their controls and those imputed with the described method.

Clustering of gene-modules

We aimed to identify groups of gene-modules that are jointly dysregulated, and to subsequently analyze their co-regulation in different patients. First M-scores for the 206 gene-modules across nine different datasets (Table 1) were calculated. In order to obtain the number of stable groups of gene-modules (k), or SLE-signatures, the matrices of M-scores from different datasets were integrated by similarity network fusion (SNF) using SNFtool R package (version 2.3.1) [28]. This process was repeated 500 times selecting different numbers of datasets (from 2 to 9) and different parameters for the SNF algorithm (number of neighbors from 10 to 30 and alpha hyperparameter from 0.3 to 0.8). Then, NbClust R package (version 3.0) was applied to obtain the best number of groups for each iteration across 30 different stability metrics [29]. Most frequently optimal number of groups obtained

among all combinations and permutations was selected as the optimal k . The process was repeated switching randomly the M-scores within each dataset to obtain the frequencies of optimal number of clusters in randomized data to discard all those results below those obtained by chance. Finally, gene-modules were grouped into k selected SLE-signatures using ConsensusClusterPlus R package (version 1.54.0) [30].

We defined the SLE-signature M-scores (M-sig) as the average of M-scores of all gene-modules grouped in the same signature (Equation 2) as a value summarizing dysregulation at signature level.

$$Msig_i = \frac{\sum_{j=1}^{n_i} (M_j)}{n_i} \quad (2)$$

where n_i is the number of gene-modules in the cluster (or signature) i and M_j is the M-score of the gene-module j .

The optimal number of subgroups of patients was also calculated on the matrix of M-scores of all patients using NbClust.

Gene-modules switching in patients during disease lifetime

We measured whether there were different and exclusive pathological mechanisms for subgroups of patients, or if highly dysregulated gene-modules switch within the same patient. For that, M-scores of patients having more than three visits from two available longitudinal datasets (Table 1) were merged. Then, the number of times each pair of gene-modules appeared strongly dysregulated in the same patient regardless the time point was counted. Pearson's chi-squared test was used to evaluate the statistical association.

Classification models for clinical variables

In order to predict drug response, clinical manifestations and other disease-related events based on gene-modules, caret R package (version 6.0–91) was used to build ML-based prediction models [22]. For each variable, 80% and 20% of patients were class-balanced and randomly selected as training and test sets (using specific datasets for the different variables to predict, see Table 1), respectively. First, to select optimal parameter, parameter tuning was performed on training set for each model by 10-fold-cross validation iterated 30 times. For binary variables, such as response or not response to a drug, different classification algorithms were tested, including Gaussian linear model, linear discriminant analysis, extreme gradient boosting, random forest, k -nearest neighbors, linear and radial super vector machine, neural networks, CART or naive bayes. For continuous variables, the previous algorithms that can be adapted for regression and some additional ones were used, such as linear model or least angle regression, covering the main ML approaches [22]. Performance results of each algorithm were measured on the test sets using different metrics, including the area under the curve (AUC),

precision, recall, F1 and the balanced accuracy [31]. The entire process was repeated 10 times from train/test selection (outer folds) and we selected as adequate variables to predict those that obtained a mean AUC (or correlation for continuous variables) greater than 0.6 across iterations with any of the algorithms. With this step, overfitting and selection bias were avoided. For each variable, the algorithm that achieved the highest mean AUC across the 10 outer folds and the model based on that algorithm with best performance were selected, as long as their AUC or correlation was greater than 0.7. [Supplementary Figure 2](#) shows a summary of the workflow for the construction of the prediction models.

Association among gene-modules and clinical variables

Association among M-scores of each gene-module and different clinical variables were measured, including clinical manifestations, comorbidities, presence/absence of auto-antibodies, levels of cytokines and blood cell type proportions, comprising 111 different clinical outcomes ([Supplementary Table 1](#)). Levels of cytokines were measured in picograms per milliliter (pg/ml) and the presence/absence of each autoantibody was measured in units/ml (with specific cutoffs for each one as it is described in Barturen *et al.* [12]). Analysis of variance test was used to measure differences in gene-modules M-scores for categorical variables and Pearson's correlation coefficients were computed for continuous variables. ML-based prediction models for each clinical variable were built.

Molecular background of disease remissions and flares

To investigate how gene-modules change at different stages of clinical disease activity, samples from the longitudinal datasets were selected having a low SLEDAI index value (SLEDAI \leq 2) and without future flares in the next 3 months. Significant changes in the proportion of patients showing a highly dysregulated gene-module or not dysregulated to the time elapsed since clinical remission were determined for each gene-module using Cox proportional-hazard models. A similar analysis was performed to measure significant changes in the proportion of patients having each gene-module highly dysregulated or not to the time until a new flare appeared, when the SLEDAI score rises above 3 and so, the disease turns clinically active. Third, we compared samples taken at the first time point of a long SLEDAI remission (samples taken after no more than 3 months of an active state of the disease and without flares during the following year) against a short drop in SLEDAI occurring between two close time points with high SLEDAI (samples taken after no more than 3 months of an active state of the disease and with a resumption of activity within 3 months). Significance was calculated using the Wilcoxon's test. Finally, ML-based predictors were built using M-scores from samples in current remission with and without

future flares (at 3 and 6 months) to predict near worsening in patients.

Drug response prediction based on M-scores

Clinical response information to Tabalumab for the patients from the GSE88887 dataset [20] was provided by Eli Lilly and Company. Clinical response was measured at Week 52 after initiation of treatment using the Systemic lupus erythematosus Responder Index-5 (SRI5). SRI5 defines as good responders those patients in whom a reduction of ≥ 5 points from baseline in SELENA-SLEDAI score is achieved, no new BILAG A or no more than one new BILAG B disease activity scores and no worsening (defined as an increase of ≥ 0.3 points from baseline) in PGA [32]. Main selection criteria for patients were the presence of antinuclear antibodies, age 18 or older with active SLE (SELENA-SLEDAI ≥ 6) and without active lupus nephritis or active central nervous system involvement. A total of 60 healthy controls, 300 placebo-treated patients and 699 Tabalumab-treated patients were collected. Patients were sampled at baseline before treatment, and at 16 and 52 weeks after treatment. First, predictive models for SRI5 response were built using the M-scores at baseline of Tabalumab-treated patients. Changes in M-scores between responder and non-responder patients at baseline, at Week 52 and over time were measured by linear models using *limma* package [33] (version 3.22.7).

Results

Gene-modules are clustered into nine main SLE-signatures

M-scores were computed for all SLE patients from nine different datasets ([Table 1](#)) with respect to their healthy controls. The consistency of the M-scores was demonstrated by selecting random subsets of healthy controls (used as reference) of different sizes in each dataset, obtaining low standard deviations of patient's M-scores even when reducing the size of controls to 10% ([Supplementary Figure 3A](#)). For clustering, we obtained high levels of stability (higher than obtained by chance) for four, six and nine gene-module clusters, renamed as SLE-signatures ([Supplementary Figure 3B](#)). Although the stability is greater for four and six clusters, nine clusters achieve a more precise grouping of related biological functions being subdivisions of clusters defined for $k=4$ and $k=6$ ([Supplementary Figure 3C](#)). The nine SLE-signatures were functionally tagged as *Plasma cell/Cell cycle*, *Neutrophil/Inflammation*, *T cell*, *NK cell*, *Interferon*, *Mitochondrion*, *Platelet*, *B cell/Plasma cell* and *Inositol metabolism* ([Supplementary Table 2](#)). [Figure 2A](#) shows the proportion of patients that present significant high M-scores for each gene-module. Non-gene-modules were always strongly dysregulated, but some modules were more frequently dysregulated than others, such as *Interferon*, *Neutrophil/Inflammation* and *Plasma cell/Cell cycle* signatures (around 70%, 20% and 20% of patients, respectively).

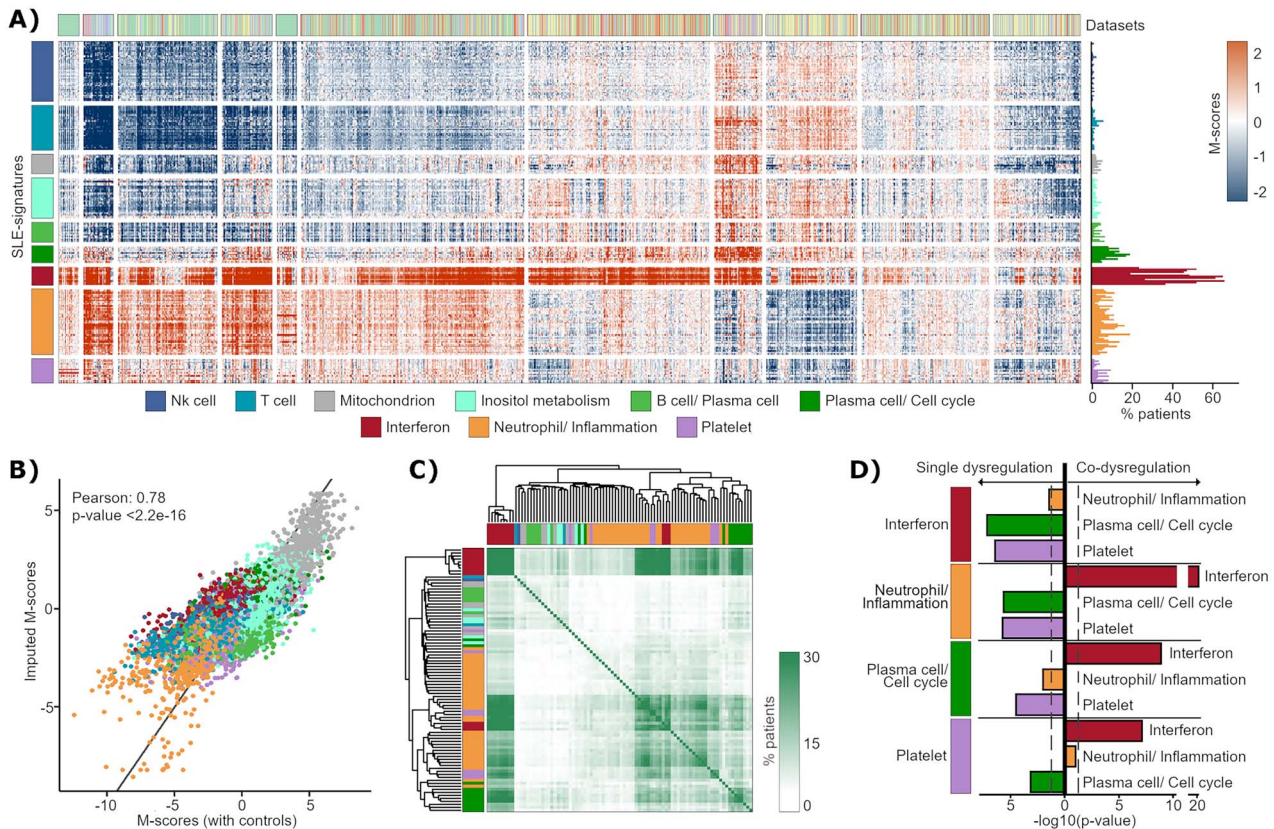


Figure 2. Clustering of gene-modules. (A) M-scores of patients from nine datasets (Table 1). Rows represent gene-modules, clustered into nine SLE-signatures, and patients are in columns. Frequency of significant dysregulated gene-modules across patients are shown to the right. (B) Correlation between M-scores from a test dataset calculated with respect to their controls and imputed by patient–patient similarity. Gene-modules are colored based on the SLE-signature in which they have been previously clustered. (C) Heatmap showing the frequency at which each pair of modules (represented in rows and columns) appears strongly and jointly dysregulated in the same patients. (D) P-values obtained comparing the proportion in which each one of the signatures (from left) is significantly dysregulated (using M-scores signification threshold) jointly with others signatures and the proportion in which it is dysregulated in isolation. The test of proportions assumes that all events occur in equal proportions (null hypothesis).

The M-scores obtained using healthy controls were compared with those obtained using patient–patient similarity (see Methods), resulting in a correlation of 0.78 between both (Figure 2B) and a P-value $<2.2 \times 10^{-16}$, demonstrating MyPROSLE can be computed, in new SLE patients, without including data from healthy controls.

SLE-signatures define two different SLE molecular subtypes

The different combinations and magnitudes of dysregulated SLE-signatures formed 11 clusters of patients (Figure 2A). Bias by dataset across clusters was not observed. Although subsequent analyzes were done at the patient level, patient stratification revealed different subtypes of patients within the disease. We found healthy-like clusters, without significant dysregulation in any SLE-signature, clusters with high M-scores in *Interferon* signature and divided mainly by gradients in *Neutrophil/Inflammation* or *Plasma cell/Cell cycle* M-scores. When a certain cluster of patients presents a high significant dysregulation in neutrophil-related modules, the plasma cell modules are not affected, and vice versa (when the clusters of patients present a high dysregulation in plasma cell modules, the neutrophil modules

do not present dysregulation) (90.37%) (Figure 2A). To delve into this point, we measured if patients always showed high dysregulation in the same gene-modules and signatures throughout the course of the disease or if, on the contrary, any module can be dysregulated at any time. Figure 2C shows the proportion of individuals from the longitudinal datasets (Table 1) for which each pair of modules appeared strongly dysregulated along available time points. Test of proportions was applied to measure the probability of finding other signatures highly dysregulated if a certain signature is highly dysregulated (Figure 2D). *Interferon* signature appeared highly co-dysregulated when *Neutrophil/Inflammation*, *Plasma cell/Cell cycle* and *Platelet* signatures were significantly dysregulated, but not vice versa. That is, *Interferon* signature can be dysregulated alone, but the rest of the signatures do so jointly with it. Again, modules related to *Neutrophil/Inflammation* signature, and the signature itself, appeared strongly dysregulated in the same patient more than 50% of the time, while the probability to find modules related to *Plasma cell/Cell cycle* signature highly dysregulated was much less in such patients during disease lifetime, and vice versa (Figure 2C). There were significant differences in the proportion of times

that *Plasma cell/Cell cycle* and *Neutrophil/Inflammation* signatures were dysregulated separately with respect to being dysregulated in the same patients (Figure 2D). *Platelet* signature was also dysregulated in the opposite direction to *Plasma cell/Cell cycle*, although it is linked to the *Neutrophil/Inflammation* signature. *Platelet* signature does not seem to be independent because very few patients had this signature highly dysregulated. As summary, these observations suggest that there are two main pathological mechanisms that differentiate patients over time, since the rest of the signatures appear combined with them. These mechanisms are associated with alterations in *Neutrophil/Inflammation* (iSLE) or in *Plasma cell/Cell cycle* (pSLE) signatures.

Association between molecular dysregulated profiles and clinical manifestations

Association between gene-modules and different types of clinical variables were measured (Supplementary Table 1). Strong significant associations between modules related to *Neutrophil/Inflammation* signature and immunological and renal manifestations, such as hematuria or proteinuria, were obtained (Figure 3A), consistent with the previous literature [15]. On the other hand, the *Plasma cell/Cell cycle* signature was associated with a very different clinical picture, mainly represented by a dermal and musculoskeletal component, such as a higher frequency of arthritis. That is, the signatures associated with iSLE (inflammatory) and pSLE (plasma cell) subtypes enriched in different manifestations. *Interferon* signature was associated with both clinical groups, with different autoantibodies (including ENA, SSA subtypes, RNP, SM, C4 and DNA antibodies (Figure 3B)), and also with IL1RA, IP10 and MCP2 cytokines (Figure 3C). Interestingly, a distinction between iSLE and pSLE subtypes when considering cytokines and autoantibodies was observed (Figure 3B–C). The *Plasma cell/Cell cycle* signature was associated with different autoantibodies, but only with one cytokine, the FAS-ligand. The *Neutrophil/Inflammation* signature was not strongly associated with any autoantibodies but with several cytokines, including BCL, IL1RA, MMP8, IL6, TGF-beta or BAFF. Thus, the *Plasma cell/Cell cycle* signature directed a disease more mediated by autoantibodies, while the *Neutrophil/Inflammation* signature did so through cytokines. It should also be noted that most cytokines associated with *Neutrophil/Inflammation* are also strongly associated with *Platelet* signature, including BAFF, TGF-Beta, IL6 and TNF-alpha.

As expected, the different SLE-signatures were strongly associated with the blood cell type they represent, such as the *Neutrophil/Inflammation* signature with a higher proportion of neutrophils (Figure 3D). On the contrary, association between plasmacytoid dendritic cells, the main interferon-producing cells and the *Interferon* signature was not observed [34]. This may be due to the fact that *Interferon* signature is composed by

the genes regulated by interferon, which are expressed almost equally in the rest of the blood cells [12, 35].

Models to predict each clinical feature were tested and a total of 57 different clinical outcomes were successfully predicted with AUC or correlation values greater than 0.7 (Figure 3E and Supplementary Table 3). It should be noted that we obtained a model with an AUC value of 0.98 to predict severe or proliferative nephritis (Supplementary Figure 4A and Supplementary Table 3), one of the most serious affections of the pathology, which is mainly diagnosed invasively by kidney biopsy. To train and test the model, we selected 30 patients from the longitudinal cohorts that did not have severe nephritis and 89 patients with biopsy-confirmed nephritis less than 1 year after/before sampling. Interestingly, *B cell/Plasma cell* and *Neutrophil/Inflammation* signatures were the most relevant signatures for the model (Supplementary Figure 4B). Significant differences in the M-scores of the signatures comparing samples with and without nephritis were obtained, being more strongly dysregulated the *Neutrophil/Inflammation*, *Interferon* and *Platelet* signatures during nephritis (Supplementary Figure 4C).

Specific dysregulations guide disease remissions and flares

We hypothesized that two samples with the same SLEDAI can be molecularly very different. For example, the transcriptome of samples with low SLEDAI would be different if the sample is taken at the beginning of a remission period or after a long-standing remission. With our system, different scenarios of clinical remission (defined as SLEDAI ≤ 2) were analyzed to extract relevant and molecular information about disease flare triggers (Supplementary Figure 5A). When remission lengthens in time, the probability of finding the *Neutrophil/Inflammation*, *B cell/Plasma cell*, *NK cell*, *Mitochondrion T cell* and *Interferon* signatures significantly dysregulated is significantly diminished (Figure 4A and Supplementary Figure 5B). This means that the M-scores of these signatures will get closer to the healthy state over time. Importantly, the signal from the *Interferon* signature takes the longest time to disappear, being still strongly dysregulated in over 25% of patients almost 300 days after clinical remission. For this reason, it is the least appropriate signature to follow-up patients' remission. This also means that interferon can be active without the patient presenting clinical manifestations (SLEDAI < 2 means not active SLEDAI clinical components), thus being likely other signatures behind the clinical worsening of the organ damage.

Next, the differences in remission time until a new flare appeared (when the SLEDAI exceeds the threshold at which the disease is considered inactive) were analyzed (Figure 4B and Supplementary Figure 5B). The closer a patient is to have a new flare, the significantly higher is the probability of finding *B cell/Plasma cell*, *Plasma cell/Cell cycle* and *T cell* signatures strongly dysregulated. This means that there are changes at the molecular level that precede a flare, before the appearance of clinical

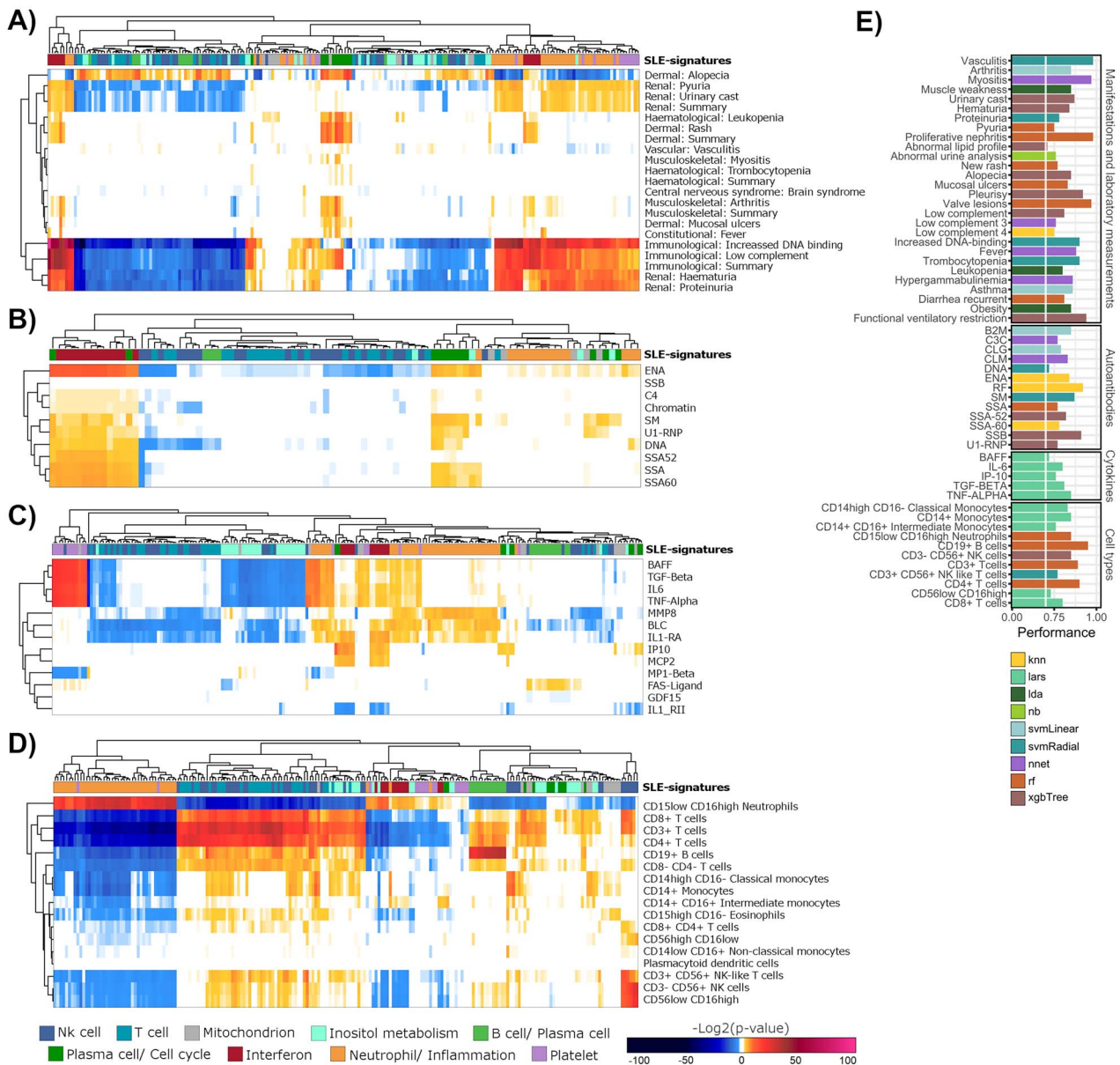


Figure 3. Associations between gene-modules and clinical variables. (A) Gene-modules and manifestation and lab measurements used in SLEDAI are represented in columns and rows, respectively. Modules are colored according to the SLE-signatures they belong to. Color ranges for heatmap entries show the P-values for each association (enrichment and depletion) in a negative logarithmic scale. Association for autoantibodies, cytokines and cell percentages is recovered in (B), (C) and (D), respectively. (E) Performance results obtained with the ML-based predictive models selected for each clinical outcome. The x-axis shows the AUC (for categorical variables) or the correlation (for numerical variables). Colors represent the algorithm selected for each model.

manifestations. M-scores of samples under remission were used to build ML models able to predict whether the patients would suffer or not a flare in the next 3 and 6 months, obtaining AUC values of 0.76 and 0.8 for naive bayes and neural network algorithms, respectively (Supplementary Table 3). That is, with our system the patients without apparent clinical manifestations but with the worst incipient prognosis can be anticipated based on molecular data.

To identify molecular patterns behind time-stable remissions, first time points of patients entering in a long SLEDAI remission (samples in remission, taken within 3 months from an active disease state and that

precede to at least 1 year of inactive disease) were compared against patients with a short drop of SLEDAI (sample in remission, taken within 3 months from an active disease state and that had a flare within the next 3 months). Significant differences at both gene-modules and signature levels were obtained, mainly related to *Neutrophil/Inflammation*, *NK cells* and *Platelet* (Figure 4C and Supplementary Figure 5C). This suggests that if the SLEDAI drop is not followed by the M-score drop of these signatures, the patient has a high probability of suffering a clinical relapse of the disease within the next 3 months. These changes were accompanied by significant differences in neutrophils and NK cells

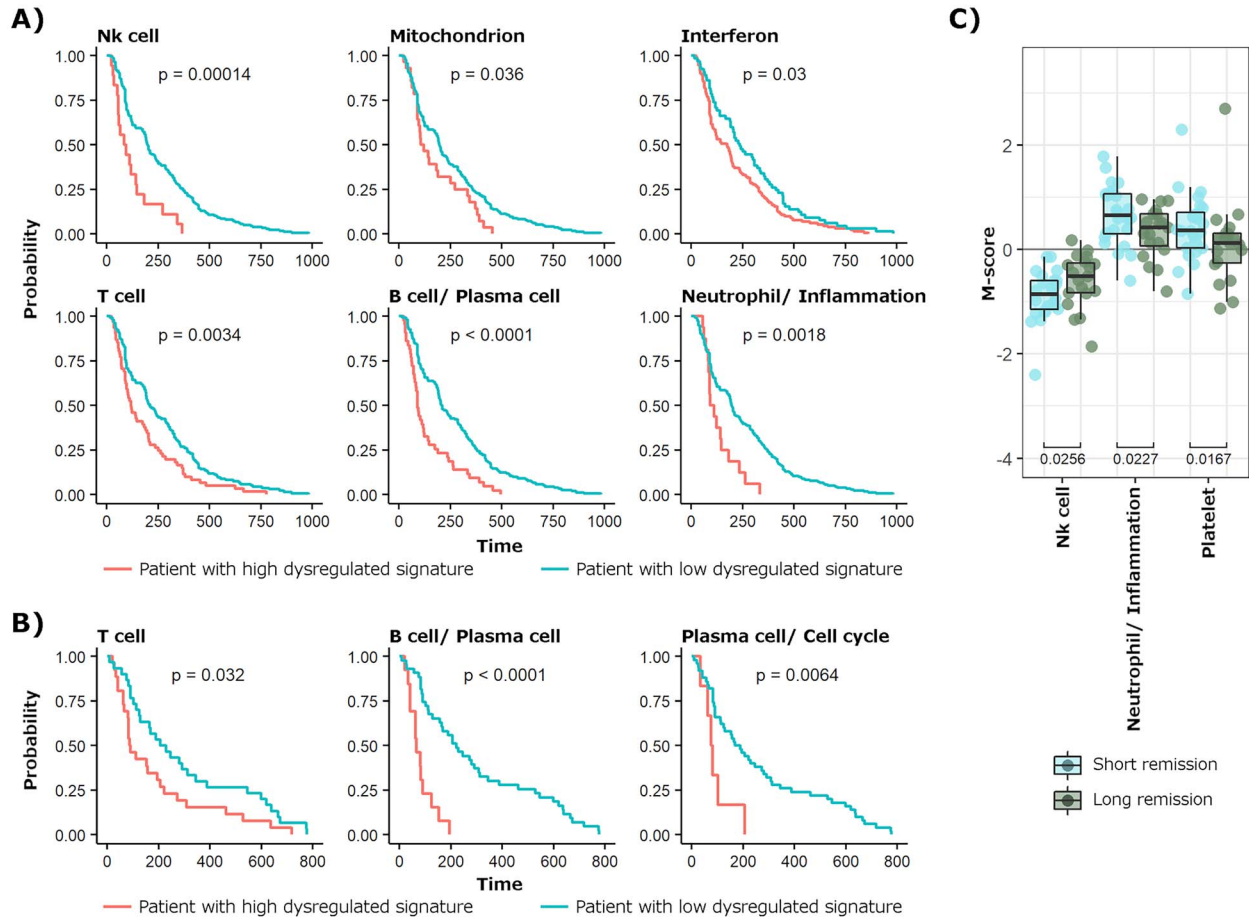


Figure 4. Molecular dysregulation behind clinical remission and flares. (A) Kaplan-Meier plots for the significant SLE-signatures obtained, where time after clinical remission is compared in patients having each signature significantly highly dysregulated (red line) versus the rest of patients (blue line). (B) The SLE-signatures are compared as a function of the time remaining until a new flare. (C) Result of comparing the SLE-signatures occurring at the first time points preceding long SLEDAI remissions against time points that represent short drops in SLEDAI occurring between active disease states.

proportions, remained higher and lower, respectively, in short drops of the SLEDAI (Supplementary Figure 5D).

MyPROSLE predicts Tabalumab response

We analyzed the effect of Tabalumab on gene-modules, a BAFF blocker that inhibits B cell maturation and differentiation into autoantibody-secreting plasma cells [36]. SRI5 response to Tabalumab at baseline based on M-scores can be predicted with high accuracy, as it is shown in Figure 5A (AUC value=0.74 and balanced accuracy = 0.7 were obtained by a neural networks-based model, Supplementary Table 3). The response prediction probabilities were significantly different comparing patients treated with Tabalumab and placebo (Figure 5B). High and low probabilities were obtained for responders and non-responders to Tabalumab, respectively, while for placebo the probabilities were distributed randomly, thus, demonstrating that our prediction model is capable of differentiating the improvements in patients caused by the drug and the improvements that occur by chance or by fluctuations in the disease itself. Figure 5C shows the average importance average for the predictive model of the genes-modules grouped by the signatures

they belong to, being B cells and plasma cells related signatures the main contributors.

Only one gene-module related to Platelet signature was significant comparing gene-modules between responders and non-responders at baseline, while at Week 52, significant differences in gene-modules related to T cell, Plasma cell/ Cell cycle and NK cell signatures were found (Figure 5D). Comparing M-scores over time between baseline and week 52, the main differences were obtained in the signatures related to B cells in both responders and non-responders. These observations are coherent with the fact that Tabalumab targets B cells (Figure 5D). Figure 5E shows SLE-signature changes on time in responders and non-responders. B cell/Plasma cell signature was significantly reduced in both groups, something that also occurred in Plasma cells/Cell cycle signature, although in less magnitude in non-responders. Interestingly, M-scores of NK cell, T cell, Mitochondrion and Inositol metabolism signatures change in the opposite way over time between responders and non-responders (Figure 5E), so they could be influencing the inefficacy of the drug in non-responder patients, directing the disease through other pathways.

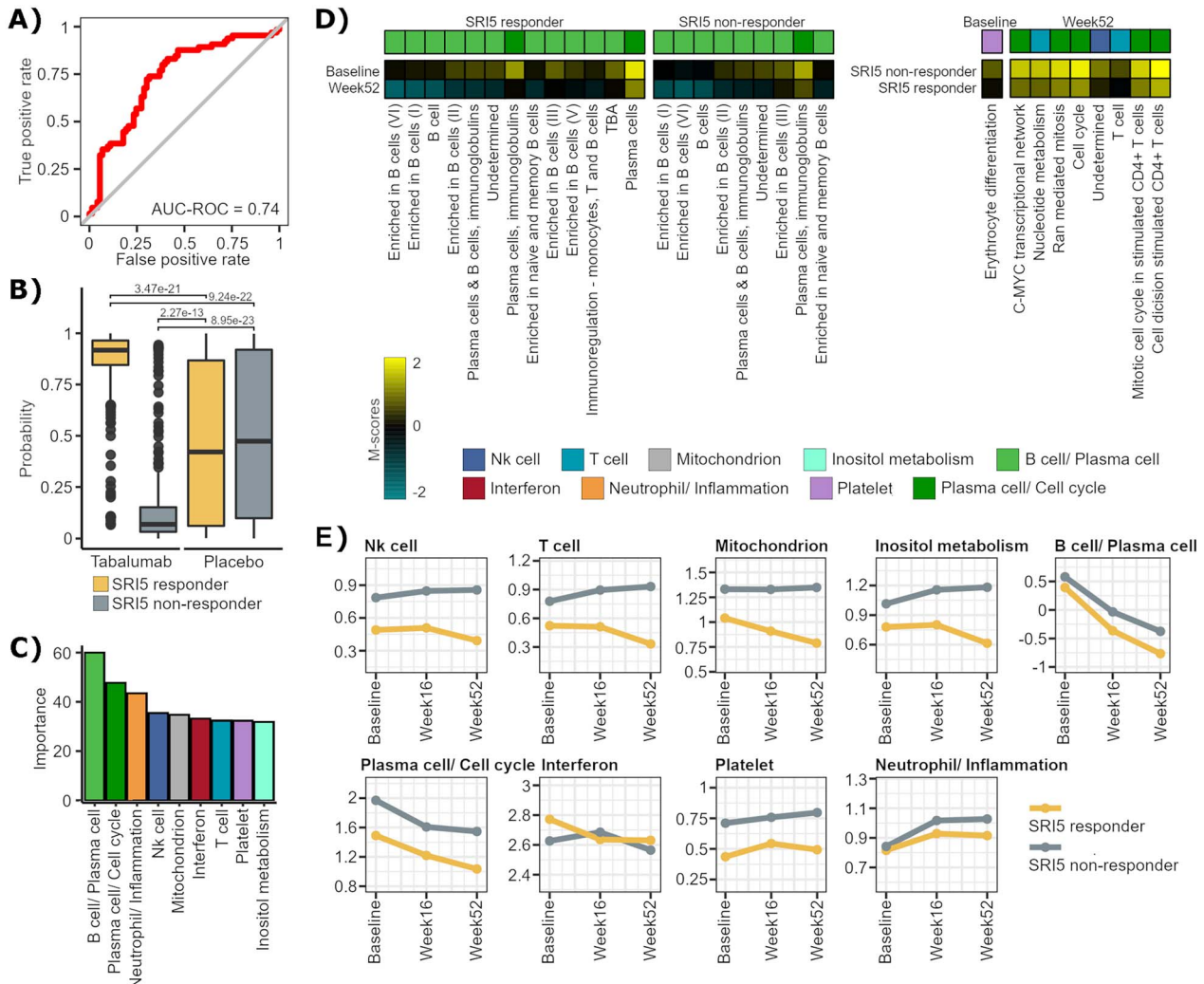


Figure 5. Tabalumab response based on M-scores. (A) ROC curve of the best predictive model for SRI5 response to Tabalumab based on M-score of patients at baseline. (B) Probabilities of SRI5 response retrieved by the predictive model for responder and non-responder patients treated with Tabalumab or with placebo. (C) Average of importance of the genes-modules for the predictive model grouped by the signatures they belong to. Importance was calculated using varImp function from caret R package. (D) The heatmaps show the mean values of the M-scores for each group of patients for each comparison. From left to right, samples from responders were compared at baseline against Week 52, non-responders were compared between the same times and then, responders and non-responders were compared at baseline and at Week 52, specifically. (E) The figure shows the mean M-scores of each signature (M-sig) and how they vary over time in responders and non-responders.

MyPROSLE implementation

The R code to calculate M-scores for all functionally annotated gene-modules is available in GitHub (<https://github.com/GENyO-BioInformatics/MyPROSLE>), including all the scripts used for each analysis described in this work. We have also included an additional R function (named M2ML, available on GitHub) that can be used to build new predictive models based on M-scores starting from gene expression data. We have also developed a web tool in which data from new patients can be loaded to perform their personalized molecular characterization and to apply the predictive models generated during this work for prediction of clinical manifestations, disease flares, autoantibodies, cytokine levels and response to Tabalumab. Figure 6 shows a summary of the web output for each of the main steps: (1) M-scores calculation

and (2) clinical outcomes prediction. MyPROSLE user interface was designed with RStudio Shiny package (version 1.7.1) [37] and it is available at <https://myprosle.genyo.es>. The tool runs on our own server with Ubuntu 20.0 operating system, 16 processors and 64 Gb of RAM memory. Some figures have been created using <https://app.biorender.com>.

Discussion

This work is structured around two main objectives: (1) the development of a new system to measure the molecular portraits of individual SLE patients (called MyPROSLE) and (2) the in-depth characterization of such molecular patterns to understand the clinical and pathological implications behind them. In the first place,

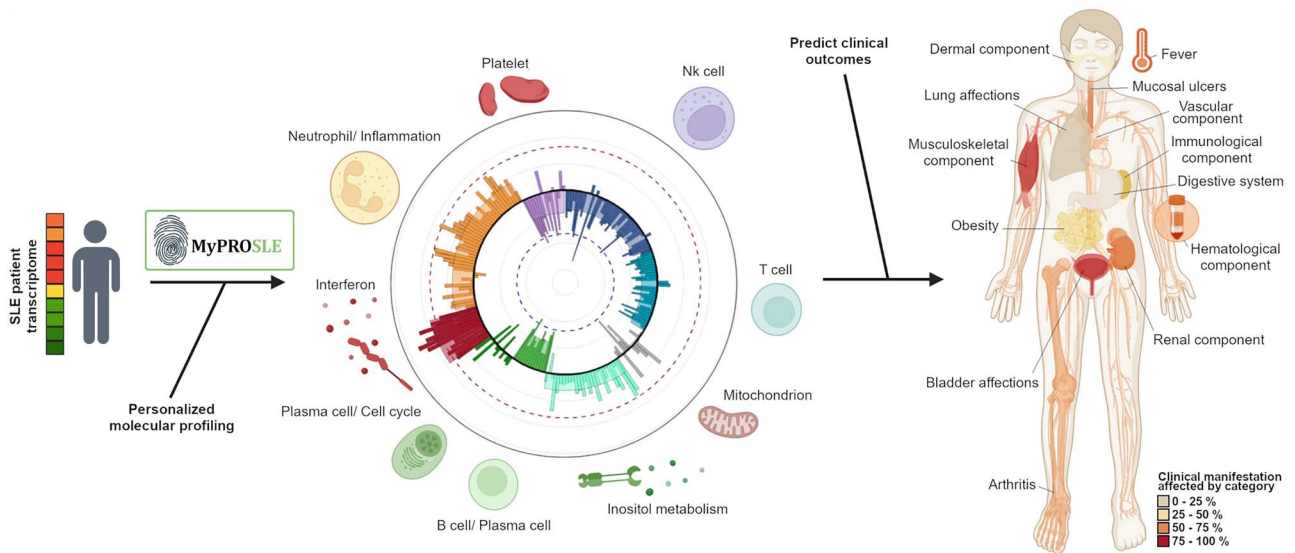


Figure 6. Web tool output example. The figure shows a summary of the web output for each of the two main steps, the personalized molecular profiling of the patients by calculating the M-scores and the clinical outcomes prediction.

the molecular state of patients can be summarized according to their dysregulation in 206 gene-modules, grouped into nine main functional signatures. MyPROSLE quantifies specific dysregulation in each patient through M-scores, so it can manage disease heterogeneity, assuming that not all patients will have the same active biological pathways throughout the disease course. M-scores are normalized values and therefore directly comparable between different studies. Although these scores initially needed a reference of healthy controls to be calculated, an additional way of calculating them has been proposed for new patients through patient-patient similarity. In this way, the M-scores can be standardized using always the same reference for their calculation.

The molecular dysregulations have also allowed to identify two well-differentiated and time-stable subtypes of SLE: an inflammatory type, iSLE, and a plasma cell type, pSLE. These subtypes have differences at the molecular and clinical level.

During the development of this work, we have demonstrated how dysregulation or its absence in certain gene-modules and signatures can provide key information from reflecting different clinical characteristics, predicting close coming flares or a better or worse response to Tabalumab. Prediction models for a total of 60 clinical outcomes were obtained (with AUC values greater than 0.7), including SLEDAI components, cytokine and auto-antibody levels, cell types proportions and comorbidities. The relationship between molecular profiles and clinical manifestations, such as the association between *Neutrophil/Inflammation* signature and kidney-related manifestations and severe nephritis [38, 39], which has been previously described, can be used in the clinic as a support to emphasize which are the risks more likely to occur in SLE patients and to be able to anticipate them. In fact, one of the potential applications is to be able

to predict proliferative nephritis, which is commonly diagnosed invasively by renal biopsy [40].

To date, some studies correlated satisfactorily clinical variables with disease activity in order to estimate disease activity [41], but studies that have tried to predict the occurrence of upcoming flares and remissions in SLE have not been successful [42]. We have obtained AUC values greater than 0.75 using the M-scores of the gene-modules to predict future flares at 3 and 6 months. In addition, signatures that precede clinical worsening have been identified and how long the signatures remain dysregulated after the patient stops having the clinical manifestations, highlighting that the Interferon signature is the one that remains active longest after clinical remission. Therefore, dysregulation of the Interferon signature is not a good marker for disease activity, as some studies previously proposed [43].

Regarding drug response, Tabalumab mainly affects the plasma cell and B cell related functions [36]. Tabalumab clinical trials failed [44], and we hypothesize that this is due to having studied all patients as a single homogeneous group. Tabalumab clinical trials failed [44], although Tabalumab shares the same target pathway as another accepted drug, Belimumab, which did meet clinical endpoints (being SRI5 the main standard endpoint) in multiple trials. We hypothesize that the trial failure is due to having studied all patients as a single homogeneous group. In this article, we have created a model that predicts the SRI5 response to the drug for individual patients (with AUC value of 0.74), a methodology that can be used to prior or select those patients who are candidates to be responders. With the appropriate data, this approach could be easily adapted for other drugs (or any clinical outcome). Indeed, we have provided R functions with which new predictive models can be created based on M-scores for new clinical outcomes starting from expression data. In addition, we

have identified the main signatures that change both after response to the drug and differentially over time between responders and non-responders, which opens the door to possible more detailed studies aimed at identifying the cause behind the non-response.

In conclusion, MyPROSLE is a powerful system to deal with the molecular heterogeneity of SLE and provides the molecular portrait of the individual patients in a standardized way, information that may be used in the future to support the choice of more effective personalized therapies and patient monitoring. MyPROSLE has been packaged within a web tool (<https://myprosle.genyo.es>), where any user can execute it in a friendly environment needing only expression data from patients, without the need of expression data from healthy controls. This workflow is easily scalable to incorporate new models for other clinical manifestations and drugs as well as for other diseases. In addition, prediction of response to Tabalumab, clinical manifestation, such as severe nephritis and disease prognosis, is provided by the web tool. Therefore, we set a precedent and an important advance in terms of personalized research oriented to a near future clinical practice within autoimmunity.

Author Contributions

All authors contributed to the analysis of the results, to the writing and the revision of the manuscript. D.T.-D. planned the entire study and actively worked on all of its subsections and wrote the manuscript. R.L.-D. handled the raw data processing and some time-related analysis. J.M.-M. set up the web application. G.B., M.M.-B. and E.C.-M. worked with clinical data from the PRECISESADS cohort. D.G. and M.P. provided clinical data from the GSE121239 cohort. P.C.-S. provided statistical support and contributed to decision making and M.E.A.-R. supervised the entire study, being a fundamental active part in the interpretation of the results. All authors reviewed the manuscript.

Key Points

- MyPROSLE allows identification and quantification of the personalized dysregulated molecular mechanisms in individual Systemic Lupus Erythematosus patients.
- Molecular portrait of a patient can be summarized into nine different functional signatures.
- We identified two subgroups of patients differentiated over time guided by *Neutrophil/ Inflammation* and *Plasma cell/ Cell cycle* signatures.
- Clinical manifestations, disease prognosis and drug responses to Tabalumab can be predicted based on molecular portrait of each patient.

Acknowledgement

We thank Eli Lilly and Company for providing us the clinical response information (SRI5) to tabalumab for the SLE

patients included in the GSE88887 dataset ([ClinicalTrials.gov](https://clinicaltrials.gov) Identifiers NCT01205438 and NCT01196091).

Funding

This project has received funding from grant PID2020-119032RB-I00 supported by MCIN/AEI/10.13039/501100011033: FEDER and the Innovative Medicines Initiative 2 Joint Undertaking (JU) under grant agreement No 831434 (3TR). The JU receives support from the European Union's Horizon 2020 research and innovation programme and EFPIA. P.C.-S.'s group is also funded by FEDER/Junta de Andalucía-Consejer'a de Transformación Económica, Industria, Conocimiento y Universidades (grants P20_00335 and B-CTS-40-UGR20). D.T.-D. is supported through the aid granted of the 'Consejería de Transformación Económica, Industria, Conocimiento y Universidades' (CTEICU), in the 2020 call, being co-financed by the European Union through the European Social Fund (ESF) named 'Andalucía se mueve con Europa', within the framework of the Andalusian ESF Operational Program 2014–2020. G.B. is supported by a Sara Borrell grant # ISCIII CD18/00149. J.M.-M. is funded by Ministerio de Universidades (Spain's Government) and the European Union – NextGenerationEU.

References

1. Goldblatt F, O'Neill SG. Clinical aspects of autoimmune rheumatic diseases. *Lancet Lond Engl* 2013;**382**:797–808.
2. Carter PJ, Lazar GA. Next generation antibody drugs: pursuit of the 'high-hanging fruit'. *Nat Rev Drug Discov* 2018;**17**:197–223.
3. Casey KA, Smith MA, Sinibaldi D, et al. Modulation of Cardiometabolic Disease Markers by Type I Interferon Inhibition in Systemic Lupus Erythematosus. *Arthritis Rheumatol* 2021;**73**:459–71.
4. Allen ME, Rus V, Szeto GL. Leveraging Heterogeneity in Systemic Lupus Erythematosus for New Therapies. *Trends Mol Med* 2021;**27**:152–71.
5. Chasset F, Arnaud L. Targeting interferons and their pathways in systemic lupus erythematosus. *Autoimmun Rev* 2018;**17**:44–52.
6. Bombardier C, Gladman DD, Urowitz MB, et al. Derivation of the SLEDAI. A disease activity index for lupus patients. The Committee on Prognosis Studies in SLE. *Arthritis Rheum* 1992;**35**:630–40.
7. Romero-Diaz J, Isenberg D, Ramsey-Goldman R. Measures of adult systemic lupus erythematosus: updated version of British Isles Lupus Assessment Group (BILAG 2004), European Consensus Lupus Activity Measurements (ECLAM), Systemic Lupus Activity Measure, Revised (SLAM-R), Systemic Lupus Activity Questionnaire for Population Studies (SLAQ), Systemic Lupus Erythematosus Disease Activity Index 2000 (SLEDAI-2K), and Systemic Lupus International Collaborating Clinics/American College of Rheumatology Damage Index (SDI). *Arthritis Care Res* 2011;**63**(Suppl 11):S37–46.
8. Sicklick JK, Kato S, Okamura R, et al. Molecular profiling of cancer patients enables personalized combination therapy: the I-PREDICT study. *Nat Med* 2019;**25**:744–50.
9. Madani Tonekaboni SA, Beri G, Haibe-Kains B. Pathway-Based Drug Response Prediction Using Similarity Identification in Gene Expression. *Front Genet* 2020;**11**:1016.

10. Franco M, Jeggari A, Peuket S, et al. Prediction of response to anti-cancer drugs becomes robust via network integration of molecular data. *Sci Rep* 2019;**9**:2379.
11. Tavakolpour S. Towards personalized medicine for patients with autoimmune diseases: Opportunities and challenges. *Immunol Lett* 2017;**190**:130–8.
12. Barturen G, Babaei S, Català-Moll F, et al. Integrative Analysis Reveals a Molecular Stratification of Systemic Autoimmune Diseases. *Arthritis Rheumatol* 2021;**73**:1073–1085.
13. Lewis MJ, Barnes MR, Blighe K, et al. Molecular Portraits of Early Rheumatoid Arthritis Identify Clinical and Treatment Response Phenotypes. *Cell Rep* 2019;**28**:2455–2470.e5.
14. Banchereau R, Hong S, Cantarel B, et al. Personalized Immunomonitoring Uncovers Molecular Networks that Stratify Lupus Patients. *Cell* 2016;**165**:551–65.
15. Toro-Domínguez D, Martorell-Marugán J, Goldman D, et al. Stratification of Systemic Lupus Erythematosus Patients Into Three Groups of Disease Activity Progression According to Longitudinal Gene Expression. *Arthritis Rheumatol Hoboken NJ* 2018;**70**:2025–35.
16. Guthridge JM, Lu R, Tran LT-H, et al. Adults with systemic lupus exhibit distinct molecular phenotypes in a cross-sectional study. *EclinicalMedicine* 2020;**20**(100291):100291.
17. Díaz-Peña R. Personalized Medicine in Autoimmune Diseases. *J Pers Med* 2021;**11**:1181.
18. Yu H, Nagafuchi Y, Fujio K. Clinical and Immunological Biomarkers for Systemic Lupus Erythematosus. *Biomolecules* 2021;**11**:928.
19. Clough E, Barrett T. The Gene Expression Omnibus database. *Methods Mol Biol Clifton NJ* 2016;**1418**:93–110.
20. Hoffman RW, Merrill JT, Alarcón-Riquelme MME, et al. Gene Expression and Pharmacodynamic Changes in 1,760 Systemic Lupus Erythematosus Patients From Two Phase III Trials of BAFF Blockade With Tabalumab. *Arthritis Rheumatol Hoboken NJ* 2017;**69**:643–54.
21. Martorell-Marugán J, López-Domínguez R, García-Moreno A, et al. A comprehensive database for integrated analysis of omics data in autoimmune diseases. *BMC Bioinformatics* 2021;**22**:343.
22. Wing MKC from J, Weston S, Williams A, et al. caret: Classification and Regression Training. 2019; <https://CRAN.R-project.org/package=caret>.
23. Li S, Roupahel N, Duraisingham S, et al. Molecular signatures of antibody responses derived from a systems biology study of five human vaccines. *Nat Immunol* 2014;**15**:195–204.
24. Chaussabel D, Quinn C, Shen J, et al. A Modular Analysis Framework for Blood Genomics Studies: Application to Systemic Lupus Erythematosus. *Immunity* 2008;**29**:150–64.
25. Weiner J, Domaszewska T. tmod: an R package for general and multivariate enrichment analysis. *PeerJ Preprints*, 2016;**4**:e2420v.
26. Menche J, Guney E, Sharma A, et al. Integrating personalized gene expression profiles into predictive disease-associated gene pools. *Npj Syst Biol Appl* 2017;**3**:1–10.
27. Bolaños AB. *Probability & Statistical Concepts: an Introduction* 1977.
28. Wang B, Mezlini A, Demir F, et al. SNFtool: Similarity Network Fusion. 2021.
29. Charrad M, Ghazzali N, Boiteau V, et al. NbClust: An R Package for Determining the Relevant Number of Clusters in a Data Set. *J Stat Softw* 2014;**61**:1–36.
30. Wilkerson MD, Hayes DN. ConsensusClusterPlus: a class discovery tool with confidence assessments and item tracking. *Bioinformatics* 2010;**26**:1572–3.
31. Larner AJ. Accuracy of cognitive screening instruments reconsidered: overall, balanced or unbiased accuracy? *Neurodegener. Dis Manag* 2022;**12**:67–76.
32. Luijten KM A C, Tekstra J, JWJ B, et al. The Systemic Lupus Erythematosus Responder Index (SRI); a new SLE disease activity assessment. *Autoimmun Rev* 2012;**11**:326–9.
33. Ritchie ME, Phipson B, Wu D, et al. limma powers differential expression analyses for RNA-sequencing and microarray studies. *Nucleic Acids Res* 2015;**43**:e47.
34. Vremec D, O’Keeffe M, Hochrein H, et al. Production of interferons by dendritic cells, plasmacytoid cells, natural killer cells, and interferon-producing killer dendritic cells. *Blood* 2007;**109**:1165–73.
35. Rönnblom L, Leonard D. Interferon pathway in SLE: one key to unlocking the mystery of the disease. *Lupus Sci Med* 2019;**6**:e000270.
36. Davidson A. Targeting BAFF in autoimmunity. *Curr Opin Immunol* 2010;**22**:732–9.
37. Chang W, Cheng J, Allaire JJ, et al. shiny: Web Application Framework for R. 2021.
38. Nishi H, Mayadas TN. Neutrophils in lupus nephritis. *Curr Opin Rheumatol* 2019;**31**:193–200.
39. Jourde-Chiche N, Whalen E, Gondouin B, et al. Modular transcriptional repertoire analyses identify a blood neutrophil signature as a candidate biomarker for lupus nephritis. *Rheumatology* 2017;**56**:477–87.
40. Rovin BH, Parikh S, Alvarado A. The Kidney Biopsy in Lupus Nephritis: Is it Still Relevant? *Rheum Dis Clin North Am* 2014;**40**:537–52.
41. Bauer JW, Baechler EC, Petri M, et al. Elevated serum levels of interferon-regulated chemokines are biomarkers for active human systemic lupus erythematosus. *PLoS Med* 2006;**3**:e491.
42. Andrade S D O, Julio PR, Nunes de Paula Ferreira D, et al. Predicting lupus flares: epidemiological and disease related risk factors. *Expert Rev. Clin Immunol* 2021;**17**:143–53.
43. Crow MK, Type I. Interferon in the Pathogenesis of Lupus. *J Immunol Baltim Md* 1950;**192**(192):5459–68.
44. Isenberg DA, Petri M, Kalunian K, et al. Efficacy and safety of subcutaneous tabalumab in patients with systemic lupus erythematosus: results from ILLUMINATE-1, a 52-week, phase III, multicentre, randomised, double-blind, placebo-controlled study. *Ann Rheum Dis* 2016;**75**:323–31.
45. Petri M, Fu W, Ranger A, et al. Association between changes in gene signatures expression and disease activity among patients with systemic lupus erythematosus. *BMC Med Genomics* 2019;**12**:4.
46. Hung T, Pratt GA, Sundararaman B, et al. The Ro60 autoantigen binds endogenous retroelements and regulates inflammatory gene expression. *Science* 2015;**350**:455–9.
47. Hu Y, Carman JA, Holloway D, et al. Development of a Molecular Signature to Monitor Pharmacodynamic Responses Mediated by In Vivo Administration of Glucocorticoids. *Arthritis Rheumatol. Hoboken NJ* 2018;**70**:1331–42.